Original Research Article

Clinical evaluation of synthetic computed tomography methods in adaptive proton therapy of lung cancer patients

Vicki Trier Taasti [a],[*], Djoya Hattu [a],[1], Stephanie Peeters [a], Anke van der Salm [a], Judith van Loon [a], Dirk de Ruysscher [a], Rasmus Nilsson [b], Sebastian Andersson [b], Erik Engwall [b], Mirko Unipan [a], Richard Canters [a]

[a] *Department of Radiation Oncology (Maastro), GROW School for Oncology and Reproduction, Maastricht University Medical Centre, Maastricht, The Netherlands*
[b] *RaySearch Laboratories AB, Stockholm, Sweden*

ARTICLE INFO

ABSTRACT

Background and purpose: Efficient workflows for adaptive proton therapy are of high importance. This study evaluated the possibility to replace repeat-CTs (reCTs) with synthetic CTs (sCTs), created based on cone-beam CTs (CBCTs), for flagging the need of plan adaptations in intensity-modulated proton therapy (IMPT) treatment of lung cancer patients.
Materials and methods: Forty-two IMPT patients were retrospectively included. For each patient, one CBCT and a same-day reCT were included. Two commercial sCT methods were applied; one based on CBCT number correction (Cor-sCT), and one based on deformable image registration (DIR-sCT). The clinical reCT workflow (deformable contour propagation and robust dose re-computation) was performed on the reCT as well as the two sCTs. The deformed target contours on the reCT/sCTs were checked by radiation oncologists and edited if needed. A dose-volume-histogram triggered plan adaptation method was compared between the reCT and the sCTs; patients needing a plan adaptation on the reCT but not on the sCT were denoted false negatives. As secondary evaluation, dose-volume-histogram comparison and gamma analysis (2%/2mm) were performed between the reCT and sCTs.
Results: There were five false negatives, two for Cor-sCT and three for DIR-sCT. However, three of these were only minor, and one was caused by tumour position differences between the reCT and CBCT and not by sCT quality issues. An average gamma pass rate of 93% was obtained for both sCT methods.
Conclusion: Both sCT methods were judged to be of clinical quality and valuable for reducing the amount of reCT acquisitions.

1. Introduction

The conformal dose distribution of proton therapy is beneficial for healthy tissue sparing, but it also makes proton therapy susceptible to anatomical changes [1]. The adaptation rate is therefore typically higher for proton therapy compared to photon therapy [2]. Plan adaptations are often seen for lung cancer patients, where several anatomical changes can happen during the course of treatment [3,4].

To ensure that the proton dose distribution is not degrading during the treatment course, repeat-CT scans (reCTs) are often acquired during the course of treatment to re-compute the treatment plan on the current patient anatomy [5]. A plan adaptation is performed on the reCT, if the dose distribution no longer fulfils the dose constraints for the target or organs-at-risk (OARs); while the treatment delivery continues without changes if the dose distribution on the reCT satisfy the dose constraints and no larger OAR dose increases are seen compared to the originally planned dose distribution [6]. However, acquisition of frequent reCTs has several disadvantages: 1) It is logistically difficult due to limited availability on the CT scanners; 2) a reCT scan is not acquired on the treatment couch and hence patient position differences as well as breathing differences may occur; 3) it exposes the patient for a high total imaging dose.

Image guidance, e.g. based on cone-beam CT (CBCT), is often used for patient positioning comparable to the positioning on the treatment

---

planning-CT (pCT) [7,8]. However, CBCTs typically have a lower image quality compared to conventional CT scans, due to larger photon scattering causing artefacts and inaccurate CT numbers, which limits the ability to re-compute the treatment plan directly on the CBCT [9].

Recently, several methods have been proposed to enhance the image quality of CBCTs [10], including scatter correction methods [11], deformable image registration (DIR) between the CBCT and the pCT [12], and deep-learning methods [13,14]. These methods have been evaluated for their ability to improve the image quality, as well as for dose computation in photon as well as proton therapy [14,15]. Such enhanced CBCT images will be referred to as synthetic CTs (sCTs).

In this study, we evaluated two sCT methods, one method based on CT number correction and one based on DIR. We performed two separate evaluations. In the primary evaluation, we assessed if the two types of sCTs flagged for plan adaptation in the same way as the weekly reCTs, i.e. if the adaptation rate was the same for the reCTs and the sCTs. This only demanded that the set of dose-volume-histogram (DVH) parameters extracted from the reCT and sCT both satisfied/dissatisfied the DVH constraints, but not necessarily that the DVH parameters were exactly the same. This evaluation we denoted *clinical evaluation*. In the secondary evaluation, we also evaluated the image quality of the sCTs by comparing proton dose computed on the sCT and the corresponding reCT. This evaluation we denoted *image quality evaluation*. The main aim of this study was to assess the possibility to reduce the amount of reCT acquisitions, by assessing if sCTs could be used to flag the need for a plan adaptation for lung cancer patients treated with intensity-modulated proton therapy (IMPT).

2. Materials and methods

2.1. Patient cohort

In total, 42 lung cancer patients clinically treated with IMPT were included (fractionation schedules: 25x2.4 Gy, 30x2 Gy, or 30x1.5 Gy). Each patient received weekly reCTs for dose assessment and daily CBCTs for patient positioning. In this study, only one reCT and one corresponding CBCT were included for each patient. The patients were divided into three groups: sixteen patients with no anatomical changes and no plan adaptation on the selected reCT in the clinical routine (group 1), twelve patients with minor anatomical changes but no plan adaptation in clinical routine on the selected reCT (group 2), and fourteen patients with anatomical changes and a plan adaptation on the selected reCT in the clinical routine (group 3).

For the clinical evaluation, the CBCT was always chosen from the same day as the reCT, to see if the adaptation decision on that particular day would be the same when assessed on the reCT and on the sCT. For the image quality evaluation, we aimed to have reCTs and CBCTs which were anatomically similar, to avoid that dose differences were caused by anatomical dissimilarities. For five patients, the anatomy was slightly different between the reCT and the same-day CBCT, due to differences in breathing pattern or posture. For these patients, another CBCT was chosen for the image quality evaluation with a few days difference to the reCT (three days at most), so the anatomy was visually similar on the reCT and CBCT.

This study was approved by the local institutional review board (approval number W 20 07 00028).

2.2. Imaging systems

The CBCT scans were acquired with the Imaging Ring (medPhoton, Salzburg, Austria). The CBCTs were acquired at either 80, 100, or 120 kVp. The pCTs and reCTs were acquired with a Siemens SOMATOM Drive or Confidence scanner (Siemens Healthineers, Forchheim, Germany) at 120 kVp. A dedicated CT conversion curve (converting CT numbers to mass density) was used for each of the two CT scanners. For the sCTs, we used the same CT conversion curve as used for the reCT

which the sCT was compared to, to exclude systematic differences in the dose computation.

The pCT and the reCT were both average CTs generated based on 4DCTs. The CBCTs were regular 3DCBCTs, but due to the longer rotation time for these acquisitions (~85 s), breathing motion was averaged in a similar manner.

2.3. Synthetic CT models

Two sCT methods were used to create sCTs based on CBCTs, developed by RaySearch Laboratories (Stockholm, Sweden). The first model was a CBCT number correction model (Cor-sCT). The second model was based on DIR between the pCT and the CBCT (DIR-sCT). Full description of the two models is given by Thing et al. [16]. All evaluations in this study were performed in a research version of RayStation 11B.

2.4. Clinical evaluation

The main aim of this study was to evaluate if the amount of reCT acquisitions could be reduced, by assessing the need for a plan adaptation on the sCT created from the CBCT. In this way, a reCT acquisition would only be needed in case a plan adaptation was required, while the reCTs which would not lead to a plan adaptation could be eliminated.

We followed our clinically reCT evaluation workflow [5] also for the sCTs. The reCT was deformably registered to the pCT, and the contours were deformably mapped from the pCT to the reCT. Similarly, the sCTs were registered to the pCT, and the contours mapped. The deformed target contours on the reCT and sCTs were checked by a radiation oncologist and edited if needed. The target contours on the reCT were checked as part of clinical routine, while the contours on the sCTs were checked as part of this study. The radiation oncologists were asked not to look at the reCT and the other sCT when checking the contours on a sCT.

Next, the clinical treatment plan was re-evaluated on the reCT/sCTs. Both the nominal dose distribution (nom) and the robust voxel-wise minimum and maximum dose distributions (VWmin/VWmax) were calculated [17]. For the robust re-evaluation, a setup uncertainty of 1 mm and a range uncertainty of 3% was used. A setup uncertainty of 5 mm was used for robustly optimization on the pCT.

The plans were clinically acceptable if the following criteria were satisfied (same criteria for pCT, reCT and sCTs): Target coverage V95%$\geq$ 95% in VWmin for all targets (i.e. primary, nodal, and metastatic), Body contour D0.03cm^3 < 115% of the prescription dose in VWmax, Mediastinal Envelope expanded by 5 mm (MedEnv_5mm) D0.03cm^3 < 66.75/76 Gy (for 25 or 30 fraction schedules, respectively) in VWmax, Spinal Cord D0.03cm^3 < 54 Gy in VWmax (this was fulfilled for all plan evaluations, and will not be mentioned in the results for the clinical evaluation) [18].

To compare the clinical decision based on the reCT and sCTs, the following outcomes were defined:

- *True negative*: Both the reCT and sCT satisfied all clinical constraints and therefore did not flag for a plan adaptation.
- *True positive*: Both the reCT and sCT did not meet one or more clinical constraints and therefore both flagged for a plan adaptation.
- *False positive*: The reCT satisfied all clinical constraints, but at least one clinical constraint was not met for the sCT whereby only the sCT flagged for a plan adaptation.
- *False negative*: One or more clinical constraints failed for reCT, but all constraints were satisfied for sCT, whereby only the reCT flagged a plan adaptation.

A false negative was seen as the most problematic result, since this would mean that the need for plan adaptation would be missed by the sCT (the reCT was seen as the ground truth). In this evaluation, the extracted DVH parameters were not compared directly, only if they satisfied the clinical constraint or not. However, to judge if potential

false negatives corresponded to minor dose difference the individual DVH parameter values were also compared.

2.5. Image quality evaluation

In the secondary evaluation, the effect of the image quality on the dose computation was assessed. To have a close match between the reCT and sCT, they were rigidly registered, and the contours were rigidly mapped from the reCT to the sCT (i.e. two different sets of contours were used for the clinical evaluation and the image quality evaluation). For this evaluation, no contour adjustment was performed (however, the reCT and CBCT were anatomically similar, as described above).

In this evaluation, a copy of the clinical treatment plan was made and a finer dose grid of $1 \times 1 \times 1$ mm^3 was used to allow for an accurate dose comparison (the clinical plan had a dose grid of $3 \times 3 \times 3$ mm^3). This fine-grid plan was re-calculated on the reCT and sCTs. Here only the nominal dose (i.e. without setup or range errors) was calculated to have a direct dose comparison, based on DVH parameters.

In addition, a 3D gamma analysis was performed between the dose on the reCT and each sCT, with a 2 mm/2% criteria and a lower dose threshold of 20% of the point maximum dose (global evaluation) in the dose distribution on the reCT. The gamma analysis was performed in Matlab 2020a (The MathWorks, Inc., Natick, MA, USA). The gamma analysis was performed both on the full dose distribution as well as the individual beam doses (3–6 beams per patient).

3. Results

Examples of the image quality of the sCTs are shown in Fig. 1.

3.1. Clinical evaluation

Two (5%) and three (7%) patients were categorised as false negatives for the Cor-sCTs and DIR-sCTs, respectively (Fig. 2). Most false positives and negatives were seen in group 2. In Table 1, the causes of the false negatives are listed. The plan was flagged for adaptation if any of the dose constraints were violated. Therefore, individual DVH parameters for a patient could be false negatives/positives without the patient being categorised as a false negative/positive; e.g. we did not require that the same dose constraint needed to be violated on the reCT and the sCT. To get the full overview, Fig. 3 shows the individual DVH parameters.

For patient 23, the over-dose seen on the reCT for MedEnv_5mm was only 0.2 Gy, while the dose on both the Cor-sCT and DIR-sCT was just below the constraint, resulting in very minor dose differences (ΔD of 0.6 Gy). Similarly, the under-dose of the nodal clinical target volume (CTVn) for patient 40 was minor. These three false negative patients were less concerning. In contrast, the results for patient 26 and 27 could be alarming, since the target coverage seen on the reCT was markedly below the clinical constraint.

3.2. Assessment of incorrectly assigned sCTs

Patients 26 and 27 were visually assessed (Fig. 4), to evaluate if there were anatomical differences between the reCT and CBCT/sCT, which could explain the large dose differences seen in Table 1. For patient 26, there was a shift of the primary tumour position between the reCT and sCT. The tumour position on the reCT differed from the pCT (not shown), causing the under-dosage on the reCT. The tumour position on the CBCT/sCT was similar to the pCT. This baseline shift of the tumour thus explained the large dose difference for this patient. The smaller
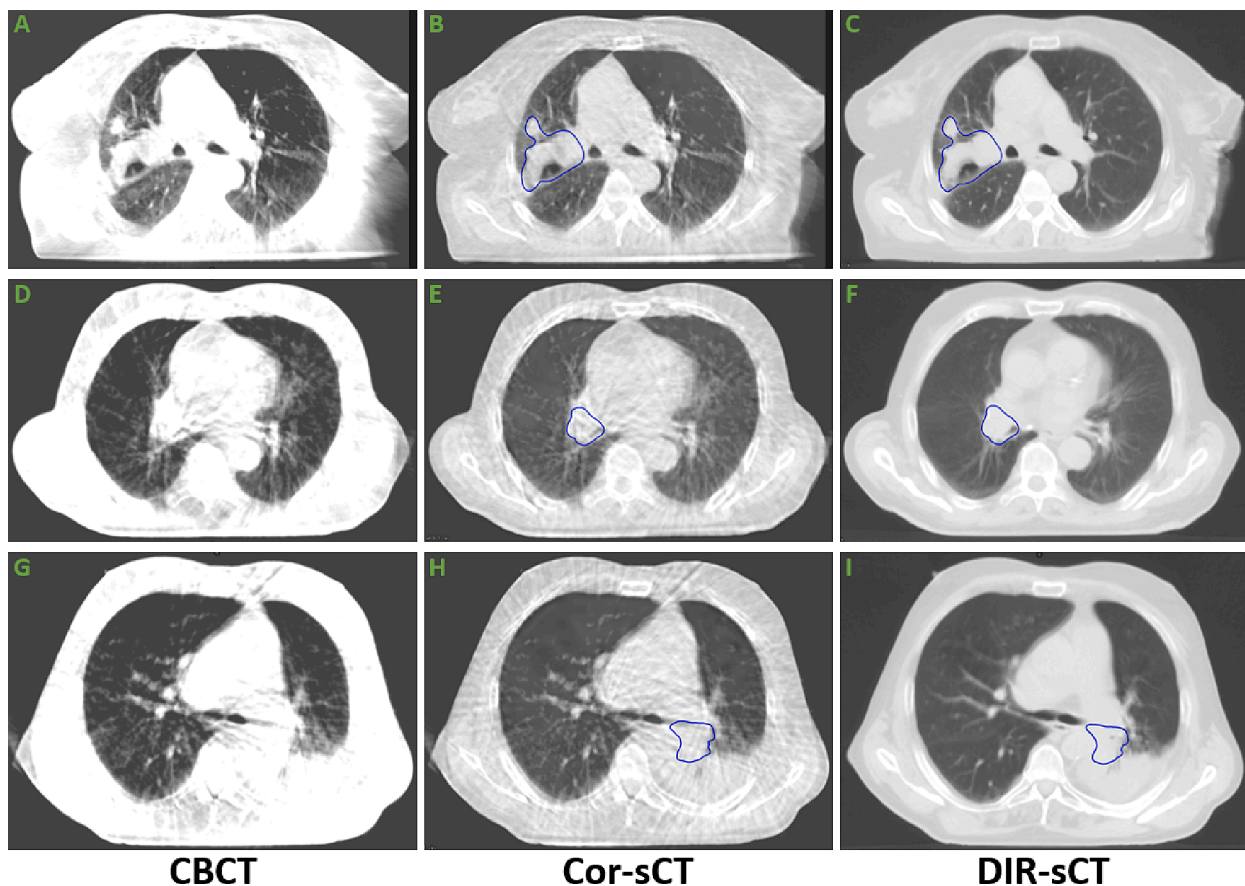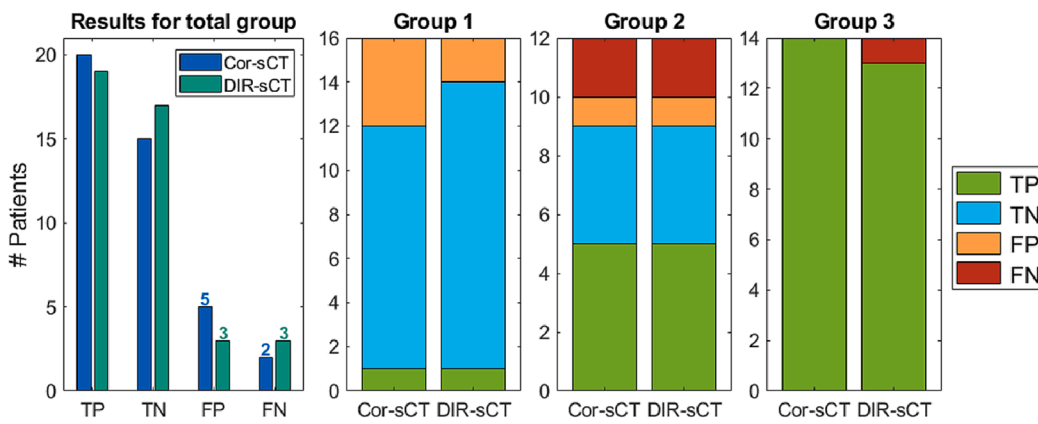

Fig. 1. Image examples of the cone-beam CTs (CBCTs), and the two synthetic CTs (sCTs). Blue contours show the primary gross tumour volume (GTVp1). No contours were delineated on the CBCTs. All images are shown in the lung window level setting (-600 HU, 1600 HU).

Fig. 2. Results of the clinical evaluation. The left bar plot shows the results for the whole patient cohort collectively. The results for each group individually are shown as stacked bar plots. Group 1: No anatomical changes; Group 2: Small anatomical changes but no plan adaptation in the clinical routine; Group 3: Anatomical changes leading to a plan adaptation in the clinical routine. *Abbreviations*: Cor-sCT – Corrected CBCT; DIR-sCT – sCT created based on deformable image registration (DIR); TP – true positive; TN – true negative; FP – false negative; FN – false negative.

Table 1

Details on the false negative synthetic CT (sCT) results. *Abbreviations*: DVH – dose-volume-histogram; reCT – repeat-CT; MedEnv_5mm – mediastinal envelope expanded by 5 mm; CTVn – nodal clinical target volume; CTVp1 – primary CTV.

Patient no. (group)	sCT type	Cause of false negative			
		DVH parameter	Constraint	DVH reCT	DVH sCT
23 (2)	Cor-sCT	MedEnv_5mm D0.03 cm^3	$\leq$66.75 Gy	67.0 Gy	66.4 Gy
23 (2)	DIR-sCT	MedEnv_5mm D0.03 cm^3	$\leq$66.75 Gy	67.0 Gy	66.4 Gy
26 (2)	Cor-sCT	CTVn V95%/ CTVp1 V95%	$\geq$95%/ $\geq$95%	94.1%/ 63.2%	99.4%/ 96.2%
27 (2)	DIR-sCT	CTVp1 V95%	$\geq$95%	86.0%	98.5%
40 (3)	DIR-sCT	CTVn V95%	$\geq$95%	93.1%	96.5%

dose difference seen for the nodal target of this patient was caused by difference in the CTVn delineation on the reCT and sCTs (not shown). For patient 27 (Fig. 4E-G), the patient posture and breathing depth differed between the CBCT/sCT and reCT. It is unknown, if this could explain the full dose difference seen between the reCT and sCTs.

3.3. Image quality evaluation

Fig. 5 shows the results of the image quality evaluation based on the dose distributions. The median of the DVH differences was close to zero in all cases. Outliers were mainly seen for the maximum doses (given as D0.03cm^3) – a slight shift of the dose distribution between the reCT and the sCT around the border of the contour could have a high impact on the maximum dose. The boxplots for the mean doses were narrow, showing that the dose distributions on the reCT and sCT were quite similar. Furthermore, the gamma pass rate was 93% for both sCT methods and for both the total dose and the individual beam dose distributions. This also shows that the shifts of the dose distribution between the reCT and the sCT were minor.

4. Discussion

In this study, we assessed two methods to create sCTs based on CBCTs, for flagging plan adaptations and re-computing dose distributions on the sCTs. For the clinical evaluation, the number of false negatives was low, which was the main criterion for the sCTs to be clinically acceptable. The number of false positives was slightly higher, showing that the sCTs did not perform exactly the same as the reCTs, but this could again potentially be due to small anatomical difference (see Fig. 3). Also, a false positive is less severe, since this flags for an

adaptation which is not needed, leading to acquisition of a reCT, which would show that the plan adaptation was not needed anyway. If the number of false positives had been high, the reduction in reCT acquisitions would be limited, and the workload for creating the sCTs would not be justified. But this was not the case in our study.

The Cor-sCTs and DIR-sCTs gave similar results for both the clinical and image quality evaluation (Figs. 1 and 5). Visually, the DIR-sCTs were a bit better (Fig. 1). However, it should be noted that the Cor-sCT represents the true anatomy as seen on CBCT, while the DIR-sCT is created by deforming the pCT to the anatomy of the CBCT and is not suitable for organ and target delineation.

In this study, we used 3DCBCT. However, for lung cancer patients, 4DCBCT might be advantageous [19–22]. DL-based methods for 4D-sCTs have also been developed [23]. The two sCT methods used in this study have also been tested on lung cancer patients for the use in photon therapy [16,24]. There, higher gamma pass rates were seen which was expected due to the higher sensitivity of dose distributions in proton therapy compared to photon therapy. DIR has also been used in an in-house built sCT method tested on paediatric proton therapy patients [25]. Deep-learning has recently attracted attention for sCT generation [13,26,27], e.g. Thummerer et al. evaluated sCTs generated applying a deep convolutional neural network on 33 thoracic cancer patients treated with proton therapy [28]. In contrast to many of these studies, we did not only focus on the accuracy of the dose computed on the sCTs, but additionally we assessed if the sCTs would have clinical benefit in our clinic by reducing the number of needed reCT acquisitions.

In this study, we only included a single CBCT, even though the patients had daily CBCTs. For the use of sCTs in the clinic, it can be discussed if the full workflow should be performed on a weekly or daily basis. A similar question was investigated by Bobić et al. for head-and-neck cancer patients [29]. In our clinic, this decision will be mainly guided by the workload this evaluation will entail. We intend to build the sCT generation and evaluation into our clinical script used for reCT evaluation [5], to automate the evaluation process, which may make daily sCT evaluation clinically feasible. In this way, the reCT could be acquired when flagged by the sCT instead of on a predefined day of the week which might be several days after an anatomical change has occurred. A similar approach is used in our photon clinic, but based on visual inspection of the CBCTs [30]. A further advantage of daily sCT evaluations would be that this could enable evaluation of the delivered dose by doing dose accumulation over the full course of treatment [31,32].

Anatomical changes and posture differences were sometimes seen between the sCT and reCT (Fig. 4). This is also a limitation we are facing in our current clinical workflow; a correct patient alignment cannot be guaranteed on the reCTs, since we do not have an image guidance system in connection with our CT scanners. For this reason, we would
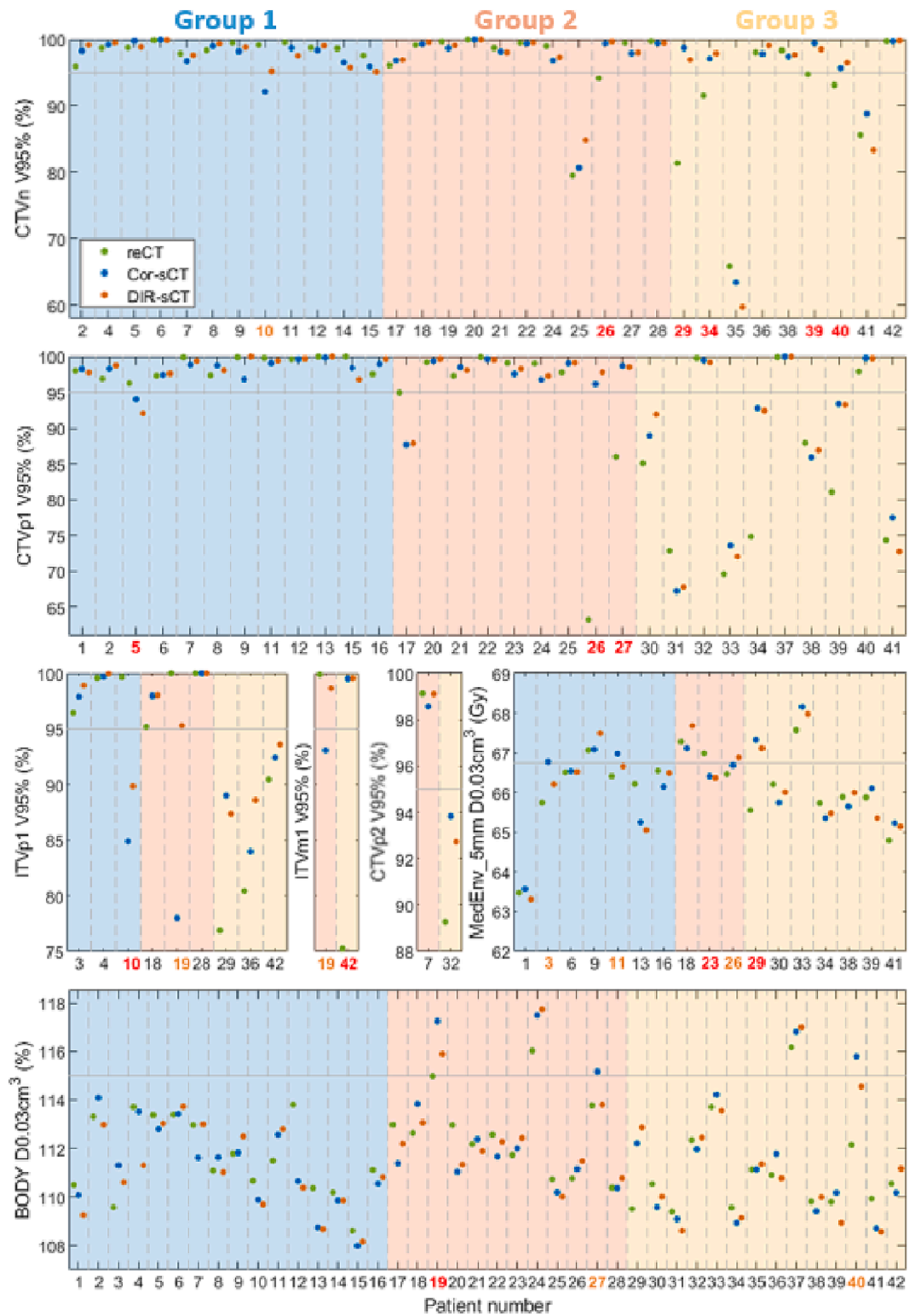
Fig. 3. Dose-volume-histogram (DVH) comparison for each of the DVH parameters evaluated for the adaptation decision (spinal cord D0.03cm^3 was also included in this evaluation, but this DVH parameter did not fail for any of these patients). The subplots for ITVp1 and ITVm1 share the y-axis. The x-axis label corresponds to the patient numbers – not all numbers are present for all subplots, since not all patients had all five target types, and for the MedEnv_5mm subplot only patients with a 25 fraction scheme were included, since the dose constraint for the 30 fraction schemes was 76 Gy, which was not exceeded for any patient. Patient numbers shown in red mark patients with a false positive or false negative DVH for both the Cor-sCT and DIR-sCT, while patient numbers shown in orange mark patient where only one of the sCTs was a false positive/negative for the given DVH parameter. *Abbreviations*: CTVn – nodal clinical target volume; CTVp1/CTVp2 – first and second primary CTV; ITVp1 – primary internal target volume; ITVm1 – metastatic ITV; MedEnv_5mm – mediastinal envelope expanded by 5 mm.
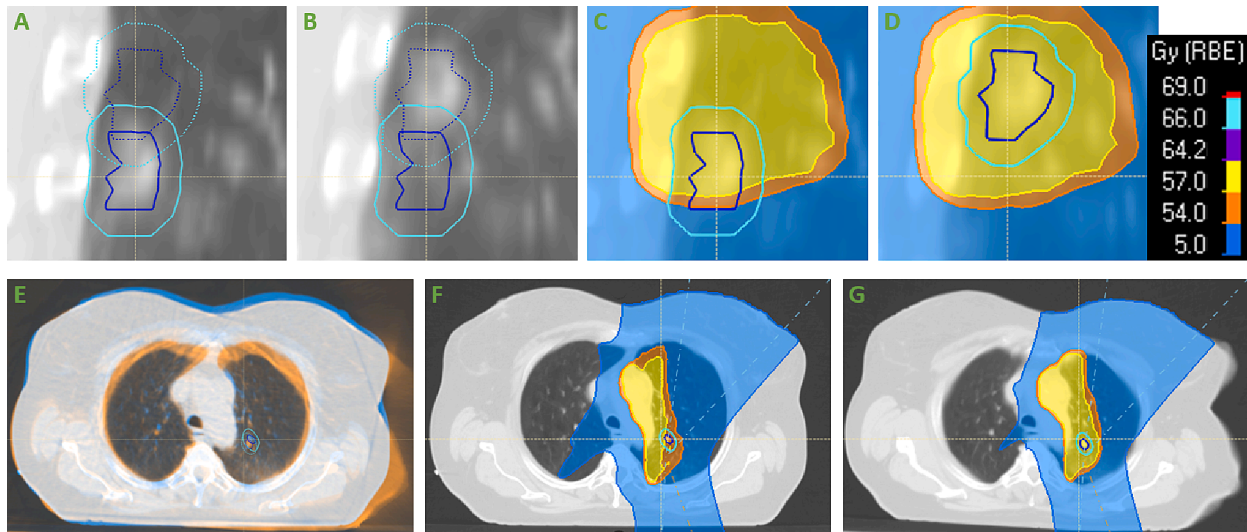
Fig. 4. Visual assessment of critical false negative patients. (A-D) Patient 26: A and C show the reCT, while B and D show the DIR-sCT (the Cor-sCT showed similar results as the DIR-sCT). The dark blue contour shows the primary gross tumour volume (GTV), while the light blue contour shows the primary clinical target volume (CTV). In A and B, the full line contours belong to the reCT, while the dotted contours belong to the DIR-sCT. The shown dose distribution is the robust voxel-wise minimum dose distribution (VWmin), as this was used for the evaluation of the target coverage. (E-G) Patient 27: E shows an image fusion of the reCT (blue) and the DIR-sCT (orange), while F and G show the VWmin on the reCT and DIR-sCT, respectively. The dose colour bar shown in the top row applies for both patients (both patients had a prescribed dose of 60 Gy).
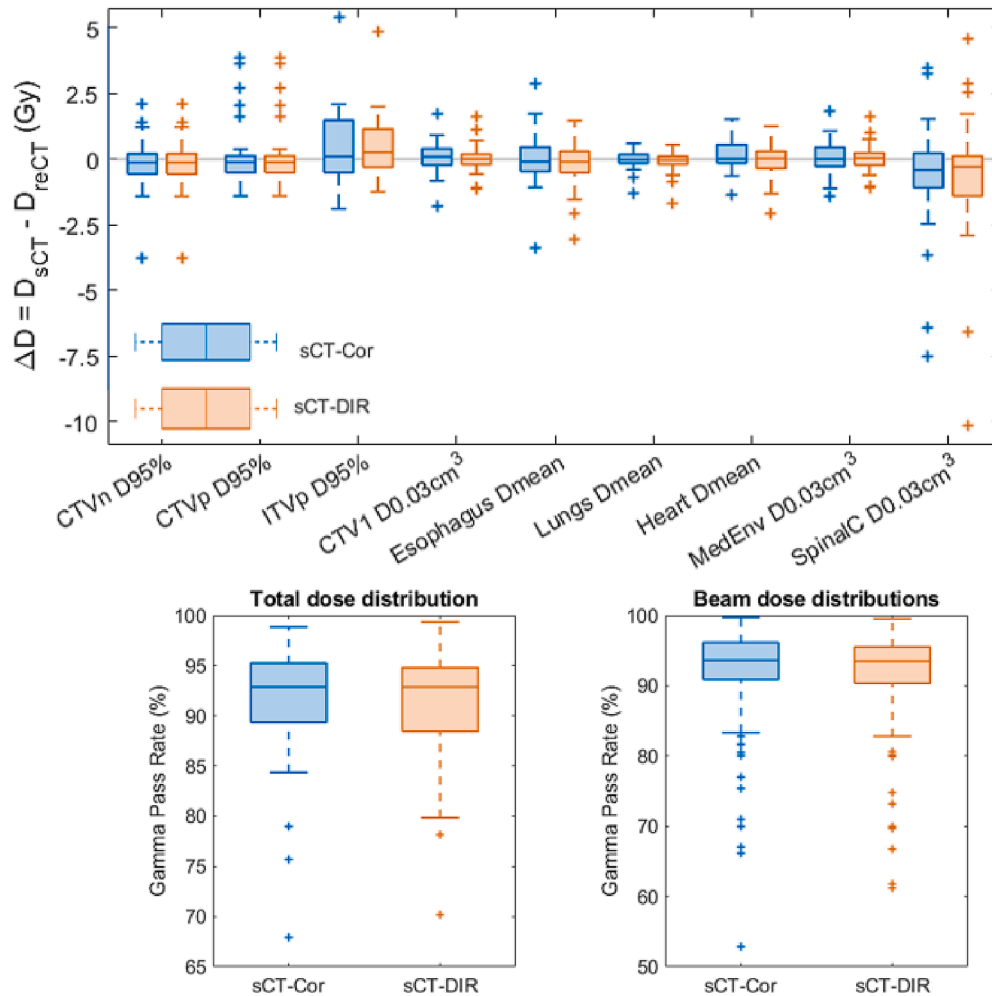

Fig. 5. Results of the image quality evaluation based on the dose re-computed on the reCT and sCTs. (Top) Dose-volume-histogram comparison. (Bottom) Gamma pass rates for 2 mm/2% criteria.

welcome the opportunity to replace the reCT evaluation with a sCT evaluation, if the dose computation accuracy is deemed satisfying, as this would remove the uncertainty of the posture differences seen between the reCT and the actual daily treatment represented by the CBCTs. This issue of reposition on the weekly reCT images was also noted by Borderías-Villarroel et al. for head-and-neck cancer patients [33].

In conclusion, we found a low number of false negatives, whereby the use of sCTs to trigger plan adaptations instead of reCTs was deemed feasible. As a first clinical use, we will replace the reCT by a sCT in the weekly reCT procedures. When the sCT flags the need for a plan adaptation, a reCT is requested to determine the actual need for adaptation. This is assumed to reduce the number of reCT acquisitions for our lung cancer patients treated with proton therapy.

Declaration of Competing Interest

The authors declare the following financial interests/personal relationships which may be considered as potential competing interests: Rasmus Nilsson, Sebastian Andersson, and Erik Engwall are employees at RaySearch Laboratories AB, Stockholm, Sweden. The rest of the authors have no conflicts of interest.

Acknowledgement

References

[1] Albertini F, Matter M, Nenoff L, Zhang Y, Lomax A. Online daily adaptive proton therapy. Br J Radiol 2020;93:20190594. https://doi.org/10.1259/bjr.20190594.

[2] Hoffmann L, Alber M, Jensen MF, Holt MI, Møller DS. Adaptation is mandatory for intensity modulated proton therapy of advanced lung cancer to ensure target coverage. Radiother Oncol 2017;122:400–5. https://doi.org/10.1016/j.radonc.2016.12.018.

[3] Møller DS, Holt MI, Alber M, Tvilum M, Khalil AA, Knap MM, et al. Adaptive radiotherapy for advanced lung cancer ensures target coverage and decreases lung dose. Radiother Oncol 2016;121:32–8. https://doi.org/10.1016/j.radonc.2016.08.019.

[4] van der Laan HP, Anakotta RM, Korevaar EW, Dieters M, Ubbels JF, Wijsman R, et al. Organ sparing potential and inter-fraction robustness of adaptive intensity modulated proton therapy for lung cancer. Acta Oncol 2019;58:1775–82. https://doi.org/10.1080/0284186X.2019.1669818.

[5] Taasti VT, Hazelaar C, Vaassen F, Vaniqui A, Verhoeven K, Hoebers F, et al. Clinical implementation and validation of an automated adaptive workflow for proton therapy. Phys Imaging Radiat Oncol 2022;24:59–64. https://doi.org/10.1016/j.phro.2022.09.009.

[6] Green OL, Henke LE, Hugo GD. Practical Clinical Workflows for Online and Offline Adaptive Radiation Therapy. Semin Radiat Oncol 2019;29:219–27. https://doi.org/10.1016/j.semradonc.2019.02.004.

[7] Nabavizadeh N, Elliott DA, Chen Y, Kusano AS, Mitin T, Thomas CR, et al. Image Guided Radiation Therapy (IGRT) Practice Patterns and IGRT's Impact on Workflow and Treatment Planning: Results From a National Survey of American Society for Radiation Oncology Members. Int J Radiat Oncol Biol Phys 2016;94:850–7. https://doi.org/10.1016/j.ijrobp.2015.09.035.

[8] Batumalai V, Holloway LC, Kumar S, Dundas K, Jameson MG, Vinod SK, et al. Survey of image-guided radiotherapy use in Australia. J Med Imaging Radiat Oncol 2017;61:394–401. https://doi.org/10.1111/1754-9485.12556.

[9] Deng L, Hu J, Wang J, Huang S, Yang X. Synthetic CT generation based on CBCT using respath-cycleGAN. Med Phys 2022;49:5317–29. https://doi.org/10.1002/mp.15684.

[10] Taasti VT, Klages P, Parodi K, Muren LP. Developments in deep learning based corrections of cone beam computed tomography to enable dose calculations for adaptive radiotherapy. Phys Imaging Radiat Oncol 2020;15:77–9. https://doi.org/10.1016/j.phro.2020.07.012.

[11] Park Y-K, Sharp GC, Phillips J, Winey BA. Proton dose calculation on scatter-corrected CBCT image: Feasibility study for adaptive proton therapy. Med Phys 2015;42:4449–59. https://doi.org/10.1118/1.4923179.

[12] Veiga C, Janssens G, Teng C-L, Baudier T, Hotoiu L, McClelland JR, et al. First Clinical Investigation of Cone Beam Computed Tomography and Deformable

[13] Maspero M, Houweling AC, Savenije MHF, van Heijst TCF, Verhoeff JJC, Kotte ANTJ, et al. A single neural network for cone-beam computed tomography-based radiotherapy of head-and-neck, lung and breast cancer. Phys Imaging Radiat Oncol 2020;14:24–31. https://doi.org/10.1016/j.phro.2020.04.002.

[14] Rusanov B, Hassan GM, Reynolds M, Sabet M, Kendrick J, Rowshanfarzad P, et al. Deep learning methods for enhancing cone-beam CT image quality toward adaptive radiation therapy: A systematic review. Med Phys 2022. https://doi.org/10.1002/mp.15840.

[15] Giacometti V, Hounsell AR, McGarry CK. A review of dose calculation approaches with cone beam CT in photon and proton therapy. Phys Med 2020;76:243–76. https://doi.org/10.1016/j.ejmp.2020.06.017.

[16] Thing RS, Nilsson R, Andersson S, Berg M, Lund MD. Evaluation of CBCT based dose calculation in the thorax and pelvis using two generic algorithms. Phys Med 2022;103:157–65. https://doi.org/10.1016/j.ejmp.2022.10.012.

[17] Korevaar EW, Habraken SJM, Scandurra D, Kierkels RGJ, Unipan M, Eenink MGC, et al. Practical robustness evaluation in radiotherapy – A photon and proton-proof alternative to PTV-based plan evaluation. Radiother Oncol 2019;141:267–74. https://doi.org/10.1016/j.radonc.2019.08.005.

[18] Taasti VT, Hattu D, Vaassen F, Canters R, Velders M, Mannens J, et al. Treatment planning and 4D robust evaluation strategy for proton therapy of lung tumors with large motion amplitude. Med Phys 2021;48:4425–37. https://doi.org/10.1002/mp.15067.

[19] Schmitz H, Rabe M, Janssens G, Bondesson D, Rit S, Parodi K, et al. Validation of proton dose calculation on scatter corrected 4D cone beam computed tomography using a porcine lung phantom. Phys Med Biol 2021;66:175022. https://doi.org/10.1088/1361-6560/ac16e9.

[20] Otter LA, Chen K, Janssens G, Meijers A, Both S, Langendijk JA, et al. Technical Note: 4D cone-beam CT reconstruction from sparse-view CBCT data for daily motion assessment in pencil beam scanned proton therapy (PBS-PT). Med Phys 2020;47:6381–7. https://doi.org/10.1002/mp.14521.

[21] Qin A, Gersten D, Liang J, Liu Q, Grill I, Guerrero T, et al. A clinical 3D/4D CBCT-based treatment dose monitoring system. J Appl Clin Med Phys 2018;19:166–76. https://doi.org/10.1002/acm2.12474.

[22] Hansen DC, Sørensen TS. Fast 4D cone-beam CT from 60 s acquisitions. Phys Imaging Radiat Oncol 2018;5:69–75. https://doi.org/10.1016/j.phro.2018.02.004.

[23] Thummerer A, Seller Oria C, Zaffino P, Visser S, Meijers A, Guterres Marmitt G, et al. Deep learning–based 4D-synthetic CTs from sparse-view CBCTs for dose calculations in adaptive proton therapy. Med Phys 2022;49:6824–39. https://doi.org/10.1002/mp.15930.

[24] Thing RS, Bernchou U, Hansen O, Brink C. Accuracy of dose calculation based on artefact corrected Cone Beam CT images of lung cancer patients. Phys Imaging Radiat Oncol 2017;1:6–11. https://doi.org/10.1016/j.phro.2016.11.001.

[25] Sheikh K, Liu D, Li H, Acharya S, Ladra MM, Hrinivich WT. Dosimetric evaluation of cone-beam CT-based synthetic CTs in pediatric patients undergoing intensity-modulated proton therapy. J Appl Clin Med Phys 2022;23. https://doi.org/10.1002/acm2.13604.

[26] Zhang Y, Yue N, Su M, Liu B, Ding Y, Zhou Y, et al. Improving CBCT quality to CT level using deep learning with generative adversarial network. Med Phys 2021;48:2816–26. https://doi.org/10.1002/mp.14624.

[27] Uh J, Wang C, Acharya S, Krasin MJ, Hua C. Training a deep neural network coping with diversities in abdominal and pelvic images of children and young adults for CBCT-based adaptive proton therapy. Radiother Oncol 2021;160:250–8. https://doi.org/10.1016/j.radonc.2021.05.006.

[28] Thummerer A, Seller Oria C, Zaffino P, Meijers A, Guterres Marmitt G, Wijsman R, et al. Clinical suitability of deep learning based synthetic CTs for adaptive proton therapy of lung cancer. Med Phys 2021;48:7673–84. https://doi.org/10.1002/mp.15333.

[29] Bobić M, Lalonde A, Sharp GC, Grassberger C, Verburg JM, Winey BA, et al. Comparison of weekly and daily online adaptation for head and neck intensity-modulated proton therapy. Phys Med Biol 2021;66:055023. https://doi.org/10.1088/1361-6560/abe050.

[30] Hattu D, Mannens J, Öllers M, van Loon J, De Ruysscher D, van Elmpt W. A traffic light protocol workflow for image-guided adaptive radiotherapy in lung cancer patients. Radiother Oncol 2022;175:152–8. https://doi.org/10.1016/j.radonc.2022.08.030.

[31] Visser SO, Ribeiro C, Dieters M, Mul VE, Niezink AGH, van der Schaaf A, et al. Robustness assessment of clinical adaptive proton and photon radiotherapy for oesophageal cancer in the model-based approach. Radiother Oncol 2022;177:197–204. https://doi.org/10.1016/j.radonc.2022.11.001.

[32] Nenoff L, Ribeiro CO, Matter M, Hafner L, Josipovic M, Langendijk JA, et al. Deformable image registration uncertainty for inter-fractional dose accumulation of lung cancer proton therapy. Radiother Oncol 2020;147:178–85. https://doi.org/10.1016/j.radonc.2020.04.046.

[33] Borderías-Villarroel E, Taasti V, Van Elmpt W, Teruel-Rivas S, Geets X, Sterpin E. Evaluation of the clinical value of automatic online dose restoration for adaptive proton therapy of head and neck cancer. Radiother Oncol 2022;170:190–7. https://doi.org/10.1016/j.radonc.2022.03.011.